Green synthesis and biological evaluation of novel 5-fluorouracil derivatives as potent anticancer agents

Farhat Jubeen[a,b], Aisha Liaqat[b], Misbah Sultan[c], Sania Zafar Iqbal[b], Imran Sajid[c] , Farooq Sher[d,*]

a. Department of Chemical and Environmental Engineering, University of Nottingham, University Park, Nottingham NG7 2RD, UK

b. Department of Chemistry, Government College Women University, Faisalabad 38000, Pakistan

c. Department of Chemistry, University of the Punjab, Lahore 54590, Pakistan

d. School of Mechanical, Aerospace and Automotive Engineering, Coventry University, Coventry CV1 5FB, UK

* Corresponding author:
Dr F. Sher
School of Mechanical, Aerospace and Automotive Engineering
Faculty of Engineering, Environment and Computing
Coventry University
Coventry
CV1 2JH
UK

Email: Farooq.Sher@coventry.ac.uk
Tel: +44 (0) 24 7765 7688

Abstract

This study reports the formation of 5-FU co-crystals with four different pharmacologically safe co-formers; Urea, Thiourea, Acetanilide and Aspirin using methanol as a solvent. Two fabrication schemes were followed i.e., solid-state grinding protocol, in which API and co-formers were mixed through vigorous grinding while in the other method separate solutions of both the components were made and mixed together. The adopted approaches offer easy fabrication protocols, no temperature maintenance requirements, no need of expensive solvents, hardly available apparatus, isolation and purification of the desired products. In addition, there is no byproducts formation, In fact, a phenomenon embracing the requirements of green synthesis. Through FTIR analysis; for API the N-H absorption frequency was recorded at 3409.02 cm^{-1} and that of –C=O is observed at 1647.77 cm^{-1}. These characteristics peaks of 5-FU were significantly shifted and recorded at 3499.40 cm^{-1} and 1649.62 cm^{-1} for 5-FU-Ac (3B) and 3496.39 cm^{-1} and 1659.30 cm^{-1} for 5-FU-As (4B) co-crystals for N-H and –C=O groups respectively. The structural differences between API and co-crystals were further confirmed through PXRD analysis. The characteristic peak of 5-FU at 2θ =28.79918º was significantly shifted in the graphs of co-crystals not only in position but also with respect to intensity and FWHM values. In addition, new peaks were also recorded in all the spectra of co-formers confirming the structural differences between API and co-formers. In addition, percent growth inhibition was also observed by all the co-crystals through MTT assay against HCT 116 colorectal cell lines *in vitro*. At four different concentrations of actinomycetes extracts i.e., 25, 50, 100 and 200 µg/mL, slightly different trends of the effectiveness of API and co-crystals were observed. However; among all the co-crystal forms, 5-FU-thiourea co-crystals obtained through solution method (2B) proved to be the most effective growth inhibitor at all the four above mentioned concentrations.

47

1. Introduction

Cancer is abnormal and uncontrolled growth and multiplication of cells. It is the second major cause of casualties each year. A number of treatment strategies and medicines have been explored and evaluated. However, none of them is producing satisfactory outcomes. Almost all the chemotherapy medicines have associated drawbacks, and studies are being carried out to minimize their side effects [1]. Chemical derivatization of an active pharmaceutical drug to mask its undesirable effects and to deliver unaltered at the site of action is a modern and fascinating approach to optimize the desired effects. The exploration of essential functionalities of heterocyclic compounds in medicinal field is a widely studied domain [2]. Certain structural features of compounds are responsible for their diverse activities[3]. Nitrogen containing heterocyclic compositions are vital components of many natural compounds e.g., antibiotics, vitamins and nucleic acids [4-7]. 5-fluorouracil (5-FU), antimetabolite of pyrimidine, a mainstream anticancer drug has been studied widely since its discovery in 1957 [4, 8]. The derivative of enone functional group in 5-FU molecule is similar to many natural and synthetic α,β-unsaturated carbonyl based compounds like chalcones, curcumin etc. responsible for antitumor activities having strong antiproliferative potential [9-11]. 5-FU administration, either intravenous, oral or topical has associated drawbacks of short plasma half-life, non-targeted cytotoxicity and other health related issues e.g., alopecia, vomiting, diarrhoea [12, 13]. For the reduction of side effects and short comes associated with 5-FU chemotherapy, 5-FU and its derivatives are under keen consideration.

Many derivatives of 5-FU have been formulated and studied following a number of different approaches. Derivatization with macromolecules e.g., carbohydrates or lipid moieties were

4

73 fabricated for crossing the membrane barriers and improving the solubility related drawbacks [14-

74 16]. Considering the fact of pH difference in different organs and tissues, a variety of pH sensitive

75 prodrugs of 5-FU has been designed for its targeted action [17]. Further working on target

76 selectivity, 5-FU modification has also been done with various DNA binders, a phenomenon

77 termed as DNA intercalation e.g., binding of DNA binder drugs to the N^1 or N^3 or at both positions

78 simultaneously [18]. Further heading towards improving drug potency of 5-FU chemotherapy with

79 no or minimum side effects, a variety of 5-FU loaded nanoparticles have been designed for

80 improving surface to volume ratio resulting in maximum drug entrapment and easy travelling to

81 targeted tissues [19-21]. Furthermore, co-crystallization of 5-FU (active pharmaceutical

82 ingredient) with co-formers is an emerging and novel phenomenon for reversible inactivation of

83 5-FU [22].

84

85 Co-crystallization of 5-FU is feasible and advantageous as it has both hydrogen bond donor and

86 acceptor groups [23]. The central focus lying behind increasing interest in this domain is easy

87 fabrication requirements i.e., designing methodologies of co-crystals are comparatively easy, no

88 requirement of costly and scarcely available instruments, feasible at room temperature, solvents

89 are required in a very low amount or sometimes solvent free methodologies can also be followed

90 [24-26]. Likewise, this phenomenon is also free from side products formation or isolation and

91 purification. As this is a very new and innovative phenomenon, there is not much work found in

92 the literature.

93

94 Successful co-crystals of 5-FU were reported with some aromatic compounds, benzoic acid

95 derivatives and heterocyclic compounds [27-29]. However, in none of the published studies, the

96   safety of co-formers regarding antimetabolites formation in the body is mentioned. Further, there

97   is no evidence of any co-crystal reported in the literature for their anticancer activity (MTT assay).

98   Most of the studies are mainly focused on the structure elucidation from the point of view of the

99   development of supra-molecular interactions. Reported literature is lacking of the data regarding

100   biological activity of the synthesized co-crystals [23, 29].

101

102   This research explains the fabrication of co-crystals of 5-FU with four different compounds i.e.,

103   urea, thiourea, acetanilide and aspirin. All the selected co-formers have hydrogen bond donor or

104   acceptor groups or both. In addition to the feasibility of supra-molecular interactions, all of these

105   four molecules manifest much significance regarding their biological activities from a

106   pharmaceutical point of view. Further, their metabolism in the body does not result in toxic

107   metabolites so, this selection of co-formers is not only safe for *in-vivo* administration but can also

108   be helpful in the improvement of 5-FU pharmacological properties [30-32]. The major elements

109   in all the selected co-formers like F, S, O, N and H are among the top ten elements in approved

110   drugs [33]. Co-crystals of 5-FU are prepared by following the solid-state grinding method and

111   solution method, with the use of methanol as a solvent. Methanol was selected considering the

112   non-reactivity of alcohols, as the OH group in alcohols as leaving group cannot be easily replaced.

113   In none of the protocols hazardous chemicals were required. Further the required apparatus was

114   economical and easily available. No by-products were formed. Co-crystals grew on ambient

115   temperature and pressure[34]. In short, both the fabrication methodologies followed in this study

116   clearly manifest and fulfil the conditions of green synthesis[35]. Formation of supra-molecular

117   interactions was evaluated through FTIR and structural differences between API and co-crystals

118   were evaluated through powdered XRD analysis of fabricated co-crystals. Comparative study of

119 API and co-crystals from the FTIR spectra proved the development of hydrogen bonding

120 interactions and the shift of characteristic 5-FU peak in PXRD graphs of co-crystals proved the

121 structural differences of 5-FU and co-formers. Furthermore, *in vitro* anticancer assays of the

122 designed crystals are also performed for their biological evaluation. All the co-crystals proved to

123 be effective for the growth inhibition of *actinomycetes* more or less than the main API. Four

124 different concentrations of *actinomycetes* were applied to variate the number of viable cells and

125 consequently the outcomes of synthesized co-crystals at different concentrations were evaluated

126 [36]. The novelty of this study over others is its analysis and identification approach for the

127 selection of the more prolific method for co-crystals fabrication from two available, under standard

128 conditions. Apart from this, the two of the synthesized co-crystals are novel, has not been

129 synthesized previously including acetanilide and aspirin's co-crystals with 5-FU. In literature, the

130 co-crystals formation was mostly confirmed through XRD analyses, but this research provides

131 strong chemical shreds of evidence of co-crystals formation by the help FTIR analyses in addition

132 to XRD analyses.

133 ## 2. Experimental

134 ### 2.1   Chemicals

135 5-FU was provided by (Sigma-Aldrich, 99%), other chemicals used in the study are urea

136 (Applichem Biochemica Chemical synthesis services, 98%), thiourea (Merck KGaA, 98%),

137 acetanilide (UNI CHEM chemical reagents, 99%) and aspirin (AnalaR chemicals Ltd. Poole

138 England). Methanol (Merck KGaA, 99.5% purity) was used to facilitate crystallization and

139 dissolution. All the chemicals were used without further purification. Co-crystals of 5-FU are

140 designed with urea, thiourea, acetanilide and aspirin following solid-state grinding method [23,

141 37] and solution method with little modification in the synthesis protocol of [38].

2.2   Synthesis of Co-crystals

2.2.1   Solid state grinding method

The calculated amounts, 4.4 mM, of API (0.572 g) and co-former (acetanilide, 0.56 g; aspirin, 0.792 g; urea, 0.24 g and thiourea, 0.32g) were weighed and mixed vigorously for about 30 minutes with the help of motor and pestle, then the ground mass was dissolved in methanol to form a solution [37]. A clear solution was obtained without heating in the case of acetanilide co-formers while in all the other three cases heating was done to get a clear solution. After the clear solution formation vials were cooled at room temperature, covered with aluminium foil and placed for crystal growth. Colourless crystals were obtained in all the four cases

2.2.2   Non- grinding solution method

The weighed amounts of API and co-formers as mentioned above were taken in 1:1 ratio, dissolved in methanol in separate vials, after that each vial was heated at water bath to get the clear solution of both the members. Then the hot solutions of API and each co former were transferred in a single vial and warmed at about 90–100 ºC for about 3 minutes, then these solutions were cooled at room temperature, covered with aluminium foil with 1 hole in it and placed in a dark cupboard for evaporation and crystal growth[38][39].

2.3   Characterisation

2.3.1   FTIR and PXRD

In order to study the changes in vibrational modes of functional groups responsible for hydrogen bonding, FTIR analysis was performed. Spectra of co-crystals were compared to the spectrum of 5-FU alone and shifting of -N-H groups and -C=O from normal peaks were evaluated to study the

163   development of non-covalent interactions for co-crystals formation[38]. The Co-crystals were

164   further evaluated through PXRD [29, 38, 40]. PXRD phenomenon is based on constructive

165   interference between monochromatic X-rays and crystalline samples. X-rays were generated by

166   cathode ray tube, filtered to get monochromatic rays, assembled to concentrate and then directed

167   towards the sample. MTT assay was performed to bio-evaluate the as prepared co-crystals [15,

168   41].

169   *2.3.2   In vitro MTT antitumor bioassay*

170   HCT 116 human colorectal cancer cell line ATCC®CCL-247™ [(catalogue no: 91091005-1VL)

171   Sigma Aldrich] was used. Cells were cultured as a monolayer in T-75 flasks Costar, followed by

172   subculturing twice a week at 37 $^{\circ}$C in 5% CO_2 and 100% relative humidity supplied incubator and

173   managed at low passage number 5 to 20. HCT 116 was cultured in McCoy's 5A medium Gibco

174   Glasgow, supplemented with 10% fetal bovine serum FBS [42], Gibco, Glasgow, UK and 1%

175   antibiotics (streptomycin, penicillin).

176

177   Adherent cells at a logarithmic growth phase were washed with 2 mL of PBS (phosphate buffered

178   saline). Afterwards detached by addition of 0.5 mL of 1X trypsin and incubated for 2–5 min at 37

179    $^{\circ}$C in the incubator. 100 µL complete growth media was added per well in 96-well flat-bottom

180   microplates. Then cells were counted for desired densities by staining with trypan blue and counted

181   with a hemacytometer. Each well was inoculated at densities of 1,000–100,000 cells per well [41].

182   Afterward cells were treated with different concentrations of actinomycete extracts such as 12 ,

183   25, 50 and 100 mg/mL. Actinomycetes, gram-positive bacteria, have been recognized as sources

184   of several secondary metabolites, antibiotics and bioactive compounds that affect microbial

185   growth. The experiment was performed in triplicates to avoid any error. Background control wells

186   containing the same volume of complete culture medium was included in each experiment along

187   with a positive control containing Triton X-100 and negative controls as well. The plate was

188   incubated at 37 °C for 24 hours in CO_2 supplied humidified incubator [43].

189

190   After 24 hours, 10 μL of 3-(4, 5-dimethyl thiazol-2-yl)-2, 5-diphenyl tetrazolium bromide (MTT)

191   was directly added in the culture media of each well. The plate was incubated for 4 hours at 37 °C

192   in 5% CO_2 incubator. After incubation plate was removed from the incubator and gently culture

193   media was removed without disturbing cells monolayer. Subsequently, 100 μL of DMSO

194   (dimethyl sulfoxide) was added in each well and plate was shaken to solubilize formazan [44].

195   Absorbance was recorded spectrophotometrically at 570 nm. The inhibitory rate was calculated

196   and plot graphs against all actinomycetes extract to evaluate their anticancer activities.

197   Subsequently, IC_{50} was calculated for each extract. The growth inhibition rate was calculated by

198   the following equation:

199
$$\% Mortality = \frac{O.D \ (control \ well) - O.D \ (treated \ well)}{O.D \ (control \ well)} \times 100$$
200

201   **3. Results and Discussion**

202   The type and the extent to which the interactions were developed between API and co-formers and

203   their biological effectiveness were evaluated through comparison of results of as synthesized co-

204   crystal with API.

3.1 Comparative analysis of the development of supramolecular interactions by FTIR spectroscopy

Spectra of all the synthesized eight co-crystals were studied in comparison to the API. The absorption frequencies of the main peaks of interest involved in hydrogen bonding interactions are arranged in Table 1. The main peaks of interest are those arising from the absorption of N-H (hydrogen bond donor) and C=O (Hydrogen bond acceptor) groups in all the spectra. In the IR spectrum of 5-FU, a blunt peak at 3409.02 cm^{-1} could be attributed to v (N-H) while a broad pointed band of high intensity at 1647.77 cm^{-1} could be attributable to absorption of C=O groups [45].

3.1.1 5-FU-U (1A and 1B)

A strong absorption peak at 3438.20 cm^{-1} and a low absorption peak at 3556.93 cm^{-1} showing hypochromic shift as compared to 5-FU in the spectrum of co-crystals of 5-FU-U obtained through grinding method were found. The peak at 3438.20 cm^{-1} in the co-crystal spectrum had shown a regular hypochromic shift in comparison to API (Fig. 5). While the other peak with a huge difference in absorption frequency and peak shape and size in comparison to 5-FU may be arisen due to the N-H groups of urea. In the other spectrum of 5-FU-U co-crystals obtained through solution method, a less pointed peak of medium intensity arose at 3437.62 cm^{-1} following the exact blue shift in absorption frequency of N-H groups of co-crystals as described in the published literature on the same phenomenon [23].

In the co-crystals of 5-FU-U, synthesized through grinding method Fig. 5 (1A), strong absorption peaks at 1633.23 cm^{-1} and 1562.88 cm^{-1} were representative of C=O absorption indicating a bathochromic shift. While in solution method, Fig. 5 (1B), 1614.94 cm^{-1} and 1559.95 cm^{-1}, could be the result of C=O absorptions. In short, for 5-FU-U co-crystals, strong red shifts for both the

228 spectra of co-crystals were observed for carbonyl group absorptions as compared to API indicating

229 the stretching of C=O bond and development of single bond character due to extensive

230 involvement of O-atoms in wander walls interactions as shown in Fig. 1. Enhanced red shifts for

231 -C=O groups absorptions in the co-crystal spectrum of solution method were indicative of

232 increased stretching of -C=O bond due to increased supramolecular interactions developing the

233 single bond character and reducing the absorption frequency in turn. This suggests the more

234 suitability of solution method than grinding method for co-crystal fabrication in this case.

235 3.1.2 5-FU-Th (2A and 2B)

236 In the case of 5-FU-Th co-crystal; from all the three peaks for N-H absorptions in co-crystal

237 spectrum of grinding method, 3599.96, 3493.97, 3376.24 cm^{-1}, and two proposed peaks, 3568.20,

238 3388.06 cm^{-1} in the spectrum of solution method (Table 1), 3493.97 and 3568.20 cm^{-1} attributable

239 to N-H groups of 5-FU were indicating the strong blue shift as compared to API according to the

240 general trend possibly due to the replacement of stronger interactions in the co-formers and API

241 alone, with the weaker interactions while forming co-crystals (Fig. 2) resulting in the less

242 stretching of N-H bond which consequently appeared as higher frequency peaks in the spectra.

243 The extra peaks might be as a result of N-H absorptions of co-formers.

244

245 In the case of 5-FU-Th co-crystals; peak at 1610.38 cm^{-1} in the spectrum of co-crystals of grinding

246 method Fig. 6 (2A) could be due to carbonyl group absorption of 5-FU, and red shift could be

247 easily justified as the development of single bond character due to Wander Walls interactions,

248 while the hypochromically shifted peak in the spectrum of solution method at 1621.81cm^{-1} is either

249 due to C=O groups or it could also be due to the absorptions of N-H scissoring vibrations as shown

250 in Fig. 6 (2A). More absorption frequency of the N-H groups of co-crystals obtained through

251 solution method Fig. 6 (2B) is in support of greater feasibility of solution method for 5-FU-Th co-

252 crystals fabrication than grinding method.

253 3.1.3 5-FU-Ac (3A and 3B)

254 In the spectrum of 5-FU-Ac co-crystals obtained through grinding method, Fig. 7 (3A), blue shift

255 was observed for the v (N-H) absorptions in co-crystals i.e., peaks were found at 3538.09 and

256 3472.57 cm^{-1} in comparison to the spectrum of API. This hypochromic effect is indicative of the

257 strengthening of N-H bond due to replacement of already present interactions with the new

258 interactions involving co-formers as shown in Fig. 3. Intermolecular hydrogen bonding

259 interactions of 5-FU (**b**) were replaced by **b*** interactions making the N-H bond more stronger and

260 shifting the absorption towards shorter wavelength i.e., at 3538.09 and 3472.57 cm^{-1} [38]. The

261 reason behind this may be the attachment of acetanilide C to electron donating methyl group which

262 consequently enhanced the N-H bond strength as compared to the C of 5-FU which was attached

263 to two inductively electron withdrawing N atoms.

264

265 Two blunt peaks were observed in the spectrum of 5-FU-Ac co-crystals obtained through solution

266 method Fig. 7 (3B) which could be attributed to N-H absorption i.e., at 3555.67 cm^{-1} and 3499.40

267 cm^{1}. Both peaks followed a hypochromic shift as compared to API. That significant change in

268 absorption frequency was indicative of major changes in the N-H interactions as explained for the

269 co-crystals obtained through the grinding method and illustrated in Fig. 3.

270

271 Carbonyl groups in the co-crystal spectrum were found to exhibit the most intense or second most

272 intense peaks in the spectra. There was significant hypochromic shift in the frequency of carbonyl

273 groups of co-crystals obtained through grinding method than that of 5-FU, indicating the alteration

13

274 of hydrogen bonding interactions of carbonyl groups in 5-FU as shown in Fig. 3, there was low

275 possibility of b* as compared to c* due to the steric hindrance of methyl group in b*. The

276 absorption frequency of carbonyl groups in the spectrum of the solution method was also slightly

277 shifted in 5-FU and co-crystals. More absorption frequency of N-H groups was indicative of more

278 strengthening of this bond following solution method as compared to grinding method for co-

279 crystal fabrication. Lower absorption frequency of carbonyl groups in the solution method was

280 indicative that the development of single bond character was more as a result of its involvement

281 in supramolecular interactions. After the discussion, the observations are leading towards the

282 development of 5-FU-Acetanilide co-crystals, solution methodology is claimed to be more

283 effective.

284 **3.1.4 5-FU-As (4A and 4B)**

285 Hypochromic shift in absorption frequencies of N-H in both the spectra of 5-FU-As co-crystals

286 was indicative of strengthening of this bond possibly owing to replacement of already present

287 interactions with weaker interactions i.e., replacement of 5-FU with aspirin molecules in the

288 neighbor resulting in more strained and less strong interactions which could be attributed to the

289 bigger molecular size of aspirin as compared to 5-FU as indicated in Fig. 4, interactions *b* could

290 be replaced by *b** and *d* could be replaced by *d**.

291

292 In the spectrum, 5-FU-As, of co-crystals through grinding method, absorption due to carbonyl

293 groups of 5-FU are not visible in the spectrum of co-crystals possibly in consequence of the

294 involvement of these carbonyl groups in supramolecular interactions and lowering of double bond

295 character due to increased stretching and single bond character of carbonyl groups of 5-FU. This

296 evidence is further supported by a strong band in 1050-1250 cm^{-1} region responsible for C-O

14

297   absorption (1242.00 cm^{-1} and 1179.10 cm^{-1}). While the absorption frequency of carbonyl group in

298   the co-crystal spectrum of solution method Fig. 8 (4B) was indicative of strong blue shift as

299   compared to that of 5-FU. It indicates the strengthening of the double bond character of C=O group

300   possibly due to the weakening of hydrogen bonding interactions of O atom as shown in Fig. 4

301   through the interactions d which could be replaced by d* and c could be replaced by c*. N-H

302   absorption peaks were almost at same positions and were of same frequency, so there was no

303   significant change in those interactions in the co-crystals obtained through both the methods. The

304   carbonyl absorption frequency was lower for the co-crystals of solution method as compared to

305   that of grinding method Fig. 8 (4A), indicating the development of single bond character resulting

306   due to the involvement of oxygen of carbonyl group in hydrogen bonding interactions. In short,

307   for the co-crystal synthesis of 5-FU-Aspirin, solution method might be more favourable than the

308   grinding method.

309

310   The hypochromic shift in absorption frequencies of N-H groups [29] in the FTIR spectras of Fig.

311   5 to Fig. 8 are indicative of strengthening of this bond possibly owing to a replacement of already

312   present interactions with weaker interactions resulting in more strained and less strong interactions

313   which could be attributed to the interference of different molecules (co-formers). These prominent

314   blue shifts in v (N-H) str cm^{-1} absorption frequencies in comparison to 5-FU were in exact

315   accordance with the shifts reported by Nadzri and co-workers [23]. Considering the 5-FU-

316   acetanilide and 5-FU-aspirin, lower absorption frequency of carbonyl groups in the solution

317   method was indicative that the development of single bond character was more as a result of its

318   involvement in supramolecular interactions. In the same way, the absorption frequencies of N-H

319 and C=O groups indicated that for the synthesis of 5-FU-Urea and 5-FU-Th, solution method might

320 be more favourable than the grinding method.

3.2 Structural differentiation of API and Co-crystals by PXRD

322 After a clear indication of more favorability of the solution method, the co-crystals formation was

323 further confirmed through powdered XRD. The shifts in the peaks of 5-FU are significant in all

324 the co-crystal forms with respect to both the shapes of the peaks and the intensity of the peaks.

325 These shifts are clearly indicative of the change in the structural characteristics of 5-FU due to the

326 change in intermolecular interactions with different co-formers [38]. From the stacked graph of

327 API and co-crystals Fig. 13, the most intense characteristic peak of 5-FU recorded at $2\theta = 28.80$

328 which is exactly equal to the value reported in the study of Goia et al. [38]. This characteristic

329 value of 5-FU seemed to be significantly shifted in the graphs of all the co-crystals. For 5-FU-U

330 (1B) co-crystals (Fig. 13), the most intense peak is recorded at $2\theta = 28.19$. The intensity of this

331 peak is much lower than that recorded for API`s characteristic peak manifesting the decreased

332 preferred orientation. It means that the arrangement of molecules in a specific orientation is not

333 appreciable. The crystal size is also not significantly bigger than the API and can be attributed to

334 the smaller size of the urea molecule. The obtained results proved the less crystallinity of the

335 synthesized co-crystals.

336

337 For 5-FU-Th (Fig. 13 2B) the most intense peak is recorded at $2\theta = 27.97$. The maximum value of

338 intensity is recorded as compared to API and all the co-crystal forms manifesting the enhanced

339 crystal packing in a specific orientation. The crystal size is also quite bigger as compared to all the

340 other cases except 5-FU acetanilide possibly due to the smaller molecule of thiourea that

341 acetanilide. Now if we talk about 5-FU- Ac co-crystals (Fig. 13 3B), the most intense peak found

16

342   at 2θ= 29.10. This peak is different from that found in the graph of API not only in the position

343   but also in its intensity and FWHM values are varied significantly, than the values recorded for 5-

344   FU (Table 4). The increase in the intensity value is indicative of the increase in the preferred

345   orientation because of enhanced crystallinity. The much smaller value of the FWHM value is

346   indicative of the significant greater size of co-crystals than API (Table 3) proving the presence of

347   both the constituents in the synthesized co-crystals. The obtained results prove the good

348   crystallinity and structural differences of co-crystals of 5-FU-Ac as compared to API obtained

349   through solution method.

350

351   The most intense peak of 5-FU-As (Fig. 13 4B) is recorded at 2θ =28.74. Although the difference

352   in 2θ value is smaller between API and co-crystals, however, the intensity of this peak is much

353   higher than that of API proving the increased crystallinity of co-crystals. The crystal size is quite

354   smaller in this case. From the above mentioned facts, the least difference in 2θ values is observed

355   between 5-FU and aspirin. However, the difference in the peak shapes, intensity and FWHM

356   values are very much different in both the API and 5-FU-As co-crystals.

357

358   For further clarity, the difference in intensities, 2θ values and FWHM values of most prominent

359   peaks are arranged in the tabular form (Table 3). In addition to the shift of 5-FU characteristic

360   peaks, there are many new peaks observed in the graphs of co-crystals and many of the other peaks

361   found in the graph of 5-FU are missing in the graphs of co-crystals. The significant differences in

362   the values and appearance of new peaks are indicative of the variations in the already present 5-

363   FU system manifesting the alterations in already present supramolecular interactions due to the

364   incorporation of different co-formers forming co-crystals. Crystallite size of all the co-crystal and

17

365   API is calculated from Scherrer equation (Table 3) [40]. Although the size difference between urea

366   and thiourea is not significant, however the crystallite size of 5-FU-Th is almost double than that

367   calculated for 5-FU-U co-crystals. This significant difference might be attributed to the most

368   compact and strong hydrogen bonding interactions in 5-FU urea co-crystals than that in the 5-FU-

369   Th co-crystals.

370

371   This effect arises due to the involvement of all the groups of urea in hydrogen bonding interactions

372   while in thiourea, sulphur in place of oxygen is not a good candidate for the development of

373   hydrogen bonding interactions leading to loose crystal packing. This is also confirmed by FTIR

374   results and from MTT assay the more anticancer potential of 5-FU thiourea co-crystals as

375   compared to 5-FU-U co-crystals also confirms the loose packing and easy release of API. In short,

376   the crystal size of all the co-crystals is also indicative of the successful formation of strong

377   hydrogen bonding interactions as all the co-crystals are significantly bigger in size than the 5-FU

378   alone manifesting the incorporation of co-formers with API, forming supramolecular synthons.

379   **3.3   Evaluation of *in vitro* Anticancer potential of co-crystals**

380   Fig. 9 to Fig. 12 explain the comparative study of the rate of % growth inhibition in relation to

381   changing the concentration of *Actinomycetes*, of the fabricated co-crystals via grinding (A) and

382   solution method (B). All the co-crystals proved to be effective for growth inhibition to a variable

383   extent against HCT 116 colorectal cell lines *in vitro*. 5-FU manifested a gradual increase in percent

384   growth inhibition with the increase in the concentration of *actinomycetes* Table 2 [41]. Its

385   maximum growth inhibition potential is 64.48% at 200 µg/mL concentration. This trend of

386   increasing growth inhibition with increasing concentration of *actinomycetes* is very much rational

387   i.e., as the concentration of microorganism's extract is increased, the drugs will have more targets

388   to act upon and consequently, the numerical values of inhibition will also increase.

389   It is obvious that in all the cases percentage growth inhibition is directly related to the

390   *actinomycetes* concentration except for 5-FU-urea co-crystals obtained through grinding method

391   (1A). For 1A co-crystals this trend is diverted from the observed trend only at 200 µg/mL i.e., for

392   1A co-crystals 100µg/mL proved to be the concentration responsible for highest growth inhibition

393   of 40.255% while in all the rest of the cases in addition to API alone 200µg/mL is the concentration

394   responsible for maximum growth inhibition as shown in Fig. 9. On the other hand, 1B co-crystals

395   of 5-FU-U has a maximum anticancer potential of 45.7195% at 200 µg/mL. The observed

396   difference in the anticancer potential of API alone and co-crystals of 5-FU-U is attributed to the

397   free and bounded conditions of 5-FU (Fig. 9).

398

399   From Table 2 it is clearly observed that the co-crystals of 5-FU-Th obtained through solution

400   method (Fig. 10 2B) are much more effective in the percent growth inhibition than that obtained

401   through grinding method Fig. 10 (2A). At all the four concentrations the anticancer potential of

402   2B co-crystals are comparable to that of 5-FU. At 25 and 200 µg/mL, the effectiveness of 2B co-

403   crystals is significantly greater than that of API alone as shown in Fig. 10. This enhanced

404   anticancer potential of 5-FU-Th co-crystals is attributed to an antioxidant potential of thiourea

405   [46]. It is clearly exhibited from Table 3, that the anticancer potential of 5-FU-Ac cocrystals

406   followed the same trend as found for 5-FU-Th co-crystals i.e., Fig. 11(3B) co-crystals are more

407   effective anticancer agents than Fig. 11 (3A) except at 100 µg/mL. Now if the API and 3B co-

408   crystals are compared, both have comparable anticancer potential at all the four concentrations

409   possibly due to the larger molecule of acetanilide consequently weaker interactions with 5-FU

410   leading to an easy release of API.

411

412   Both the cocrystals of 5-FU-As follow the general trend of increasing growth inhibition with

413   increasing *actinomycetes* concentration however; this is the only co-former in this study whose

414   Fig. 12(4A), grinding method co-crystals exhibited greater anticancer potential than 4B (Solution

415   method). Aspirin`s own anticancer potential [30] made the 4A co-crystals almost as effective as

416   API at all the concentrations of actinomycetes. The lesser effectiveness of 4B co-crystals can be

417   justified by the stronger hydrogen bonding interactions of 4B co-crystals than 4A as evidenced

418   from FTIR results leading to a slower release of API (Fig. *12*). If we consider the comparative

419   response of all the co-crystals and API at individual concentrations, the following trends were

420   observed in the order of decreasing effectiveness.

421

422   At 25 µg/mL, and 200 µg/mL, 5-FU-Th (Fig. 10) co-crystals obtained through solution method

423   (2B) proved to be the co-crystals responsible for maximum growth inhibition as shown in Table 2

424   While at 50 µg/mL and 100 µg/mL API alone was the best suited growth inhibitor. Increasing

425   *actinomycetes* (target) concentrations increased the subsequent growth inhibition. However, the

426   rate of increase is different for all the co-formers due to the different nature of all the co-formers.

427   The best outcomes of co-crystals like 5-FU-Th regarding MTT assay might be attributed to the

428   readily release of the API and increased effectiveness as compared to 5-FU are supposed to be due

429   to the individual pharmaceutical effectiveness of co-formers [47].

430

431 As all the selected co-formers have their own proved pharmaceutical significance [30, 46], so these

432 changes in the activity of 5-FU after the formation of co-crystals very much rational and these

433 trends might be attributed to the individual properties of all the co-formers. From the obtained

434 results, it could be inferred that the solution method might be the favourable one for the maximum

435 growth inhibition especially in the case of 5-FU-Th (2B) and 5-FU-Ac (3B) co-crystals, confirms

436 from Fig. 10 and Fig. 11. To the best of our knowledge, MTT assays are not reported in any

437 published study on 5-FU co-crystals. Nadzri and co-workers [23] reported anticancer activities of

438 the synthesized co-crystals but the author focused on the binding affinities of co-crystals with

439 targeted protein, not on the percent growth inhibition. In another study, Dai et al. [29], focused on

440 the membrane permeability of synthesized cocrystals. So, this is the first time in this study, MTT

441 assays of synthesized co-crystals were performed and all the eight synthesized co-crystals proved

442 to be effective from the obtained results.

443

444 In addition to the evidences of cocrystal formation through hydrogen bonding interactions and

445 structural verification and its biological effectiveness with the help of their *in vitro* cytotoxic

446 evaluation, it is important to add the significance and feasibility of the methodologies opted for

447 the synthesis. The marvellous phenomenon of green chemistry was the aim behind the selection

448 of both the protocols to carry out the synthesis in the environment friendly way with maximum

449 output. The apparatus and chemicals used were easily available and economical. All the chemicals

450 used were nonhazardous required in very low amount [48]. Further the selected co-formers were

451 also not expensive. All the co-crystals developed at ambient temperature and pressure[34]. The

452 product gain in all the eight cases was maximum as there was no byproducts formation evidenced

453 visually or through FTIR and PXRD analysis. As there was no byproduct formation, therefore,

454   there was no stress to getting rid of waste byproducts at the end of the synthesis. In short, the whole

455   synthesis process complies the rules of green chemistry devised by IUPAC [49].

4. Conclusions

457   Eight different co-crystals were prepared. All four co-formers were selected after a keen study on

458   their pharmacological properties and subsequent metabolites. The successful co-crystals were

459   formed at room temperature following both the methodologies, also supported by PXRD and FTIR

460   results. Through both, the characterization techniques, significant shifts in the anticipated peaks of

461   5-FU were observed as the spectra of API and co-crystals were studied in comparison. In all the

462   FTIR spectra of co-crystals, the main peaks of interest that are –N-H (3409.02 cm^{-1}) and –C=O

463   (1647.77 cm^{-1}) were significantly shifted than the spectrum of 5-FU following the same trend

464   reported in the literature. Through PXRD, the most intense characteristic peak of 5-FU is at 2θ=

465   28.79918°. This peak is not only shifted in position in all the graphs of co-crystals but also in

466   intensity and FWHM values. Moreover, the appearance of new peaks in the graphs of co-crystals

467   in comparison to API proved the formation of new molecules. 5-FU-Ac co-crystals and 5-FU-Th

468   co-crystals obtained through solution method proved to be the co-crystals with the highest trend

469   of preferred orientation and increased crystallinity. MTT assay proved that all the co-crystals

470   manifested their activity against HCT 116 colorectal cell lines. Through anticancer results, again

471   the 5-FU-Ac and 5-FU-Th co-crystals obtained through solution method proved to be the best

472   agents for maximum growth inhibition, agreeing with the result of FTIR and PXRD. In short, this

473   study is based on the very novel and the new phenomenon of co-crystallization. Due to its

474   simplicity, cost-effectiveness, easy fabrication protocols, no by-products formation and successful

475   derivatization of API, this phenomenon may prove to be effective for future discoveries in cancer

476   treatment. After the method optimization and estimation of anticancer potential of these co-

477   crystals, the as prepared supramolecular synthons can be further bio-evaluated for the estimation

478   of their *invivo* safety. Moreover; working in the same line many effective co-formers can also be

479   studied for their contribution in the anticancer domain that is actually the need of the hour.

References

1. Zhang, X., et al., Podophyllotoxin derivatives as an excellent anticancer aspirant for future chemotherapy: A key current imminent needs. Bioorg Med Chem, 2018. 26(2): p. 340-355.

2. Zha, G.F., et al., Pharmaceutical significance of azepane based motifs for drug discovery: A critical review. Eur J Med Chem, 2019. 162: p. 465-494.

3. Zhao, C., et al., Arylnaphthalene lactone analogues: synthesis and development as excellent biological candidates for future drug discovery. RSC Advances, 2018. 8(17): p. 9487-9502.

4. Jubeen, F., et al., Eco-friendly synthesis of pyrimidines and its derivatives: A review on broad spectrum bioactive moiety with huge therapeutic profile. Synthetic Communications, 2018. 48(6): p. 601-625.

5. Rakesh, K.P., et al., Benzisoxazole: a privileged scaffold for medicinal chemistry. Medicinal Chemistry Commumications, 2017. 8: p. 2023-2039.

6. Moku, B., et al., The significance of N-methylpicolinamides in the development of anticancer therapeutics: Synthesis and structure-activity relationship (SAR) studies. Bioorg Chem, 2019. 86: p. 513-537.

7. Wang, M., et al., Amino acids/peptides conjugated heterocycles: A tool for the recent development of novel therapeutic agents. Bioorg Chem, 2018. 76: p. 113-129.

8. Carrillo, E., et al., 5-Fluorouracil derivatives: a patent review (2012–2014). Expert opinion on therapeutic patents, 2015. 25(10): p. 1131-1144.

9. Qin, H.L., et al., Synthesis of alpha,beta-Unsaturated Carbonyl-Based Compounds, Oxime and Oxime Ether Analogs as Potential Anticancer Agents for Overcoming Cancer Multidrug Resistance by Modulation of Efflux Pumps in Tumor Cells. J Med Chem, 2016. 59(7): p. 3549-61.

10. Qin, H.L., et al., Synthesis and mechanistic studies of curcumin analog-based oximes as potential anticancer agents. Chem Biol Drug Des, 2017. 90(3): p. 443-449.

11. Zha, G.F., et al., Discovery of potential anticancer multi-targeted ligustrazine based cyclohexanone and oxime analogs overcoming the cancer multidrug resistance. Eur J Med Chem, 2017. 135: p. 34-48.

24

509   12.   Radwan, A.A. and F.K. Alanazi, Design and synthesis of new cholesterol-conjugated 5-
510   fluorouracil: a novel potential delivery system for cancer treatment. Molecules, 2014.
511   19(9): p. 13177-13187.

512   13.   Miura, K., et al., 5-fu metabolism in cancer and orally-administrable 5-fu drugs. Cancers,
513   2010. 2(3): p. 1717-1730.

514   14.   Zhang, Q., et al., New utilization of Polygonum multiflorum polysaccharide as
515   macromolecular carrier of 5-fluorouracil for controlled release and immunoprotection. Int
516   J Biol Macromol, 2018. 116: p. 1310-1316.

517   15.   Petaccia, M., et al., Correction: Inclusion of new 5-fluorouracil amphiphilic derivatives in
518   liposome formulation for cancer treatment. MedChemComm, 2016. 7(2): p. 378-378.

519   16.   Köksal Karayildirim, Ç., et al., Formulation, characterization, cytotoxicity and
520   Salmonella/microsome mutagenicity (Ames) studies of a novel 5-fluorouracil derivative.
521   Saudi pharmaceutical journal : SPJ : the official publication of the Saudi Pharmaceutical
522   Society, 2018. 26(3): p. 369-374.

523   17.   Ofonime Udofot, K.A., Bridg'ette Israel, and Edward Agyare, Cytotoxicity of 5-
524   fluorouracil-loaded pH-sensitive liposomal nanoparticles in colorectal cancer cell lines.
525   Integr Cancer Sci Ther, 2015. 2(5): p. 245–252.

526   18.   Zhou, G., et al., Aspirin hydrolysis in plasma is a variable function of butyrylcholinesterase
527   and platelet-activating factor acetylhydrolase 1b2 (PAFAH1b2). J Biol Chem, 2013.
528   288(17): p. 11940-8.

529   19.   Tummala, S., Kumar, MNS., Prakash, A Formulation and characterization of 5-
530   Fluorouracil enteric coated nanoparticles for sustained and localized release in treating
531   colorectal cancer. Saudi Pharmaceutical Journal, 2015. 23(3): p. 308-314.

532   20.   Subudhi, M.B., et al., Eudragit S100 coated citrus pectin nanoparticles for colon targeting
533   of 5-fluorouracil. Materials, 2015. 8(3): p. 832-849.

534   21.   Dong, P., et al., Innovative nano-carriers in anticancer drug delivery-a comprehensive
535   review. Bioorg Chem, 2019. 85: p. 325-336.

536   22.   Stoler, E. and J. Warner, Non-covalent derivatives: Cocrystals and eutectics. Molecules,
537   2015. 20(8): p. 14833-14848.

538   23.   Nadzri, N.I., et al., 5-fluorouracil co-crystals and their potential anti-cancer activities
539   calculated by molecular docking studies. Journal of Chemical Crystallography, 2016.
540   46(3): p. 144-154.

541   24.   Douroumis, D., S.A. Ross, and A. Nokhodchi, Advanced methodologies for cocrystal
542   synthesis. Advanced Drug Delivery Reviews, 2017. 117: p. 178-195.

543   25.   Karimi-Jafari, M., et al., Creating Cocrystals: A Review of Pharmaceutical Cocrystal
544   Preparation Routes and Applications. Crystal Growth & Design, 2018. 18(10): p. 6370-
545   6387.

546   26.   Likhitha, U., et al., Do hydrogen bonding and noncovalent interactions stabilize
547   nicotinamide-picric acid cocrystal supramolecular assembly? Journal of Molecular
548   Structure, 2019. 1195: p. 827-838.

549   27.   Delori, A., M.D. Eddleston, and W. Jones, Cocrystals of 5-fluorouracil. CrystEngComm,
550   2013. 15(1): p. 73-77.

551   28.   Mohana, M., P.T. Muthiah, and C.D. McMillen, Supramolecular hydrogen-bonding
552   patterns in 1:1 cocrystals of 5-fluorouracil with 4-methylbenzoic acid and 3-nitrobenzoic
553   acid. Acta Crystallogr C Struct Chem, 2017. 73(Pt 3): p. 259-263.

554   29.   Dai, X.-L., et al., Improving the Membrane Permeability of 5-Fluorouracil via
555   Cocrystallization. Crystal Growth & Design, 2016. 16(8): p. 4430-4438.

556   30.   Langley, R.E. and P.M. Rothwell, Potential biomarker for aspirin use in colorectal cancer
557   therapy. Nature Reviews Clinical Oncology, 2012. 10: p. 8.

558   31.   Li, J.P., et al., Quantitative determination of five metabolites of aspirin by UHPLC-MS/MS
559   coupled with enzymatic reaction and its application to evaluate the effects of aspirin dosage
560   on the metabolic profile. J Pharm Biomed Anal, 2017. 138: p. 109-117.

561   32.   Rakesh, K.P., et al., Synthesis and SAR studies of potent H+/K+-ATPase and anti-
562   inflammatory activities of symmetrical and unsymmetrical urea analogues. Medicinal
563   Chemistry Research, 2017. 26(8): p. 1675-1681.

564   33.   Fang, W.Y., et al., Synthetic approaches and pharmaceutical applications of chloro-
565   containing molecules for drug discovery: A critical review. Eur J Med Chem, 2019. 173:
566   p. 117-153.

567   34.   Ahmed, S., et al., A review on plants extract mediated synthesis of silver nanoparticles for
568   antimicrobial applications: A green expertise. J Adv Res, 2016. 7(1): p. 17-28.

569   35.   Ansari, M.D., et al., Organo-nanocatalysis: An emergent green methodology for construction of bioactive oxazines and thiazines under ultrasonic irradiation. Journal of Molecular Structure, 2019. 1196: p. 54-57.

572   36.   Suthindhiran, K. and K. Kannabiran, Cytotoxic and Antimicrobial Potential of Actinomycete Species Saccharopolyspora salina VITSDK4 Isolated from the Bay of Bengal Coast of India American Journal of Infectious Diseases 2009. 5(2): p. 90-98.

575   37.   Sonawane, R.P., Green synthesis of pyrimidine derivative. International Letters of Chemistry, Physics and Astronomy, 2014. 2: p. 64-68.

577   38.   Moisescu-Goia, C., M. Muresan-Pop, and V. Simon, New solid state forms of antineoplastic 5-fluorouracil with anthelmintic piperazine. Journal of Molecular Structure, 2017. 1150: p. 37-43.

580   39.   Yan, X., et al., Synthesis and structure–antitumor activity relationship of sulfonyl 5-fluorouracil derivatives. Phosphorus, Sulfur, and Silicon, 2009. 185(1): p. 158-164.

582   40.   Li, S., J.-M. Chen, and T.-B. Lu, Synthon polymorphs of 1: 1 co-crystal of 5-fluorouracil and 4-hydroxybenzoic acid: their relative stability and solvent polarity dependence of grinding outcomes. CrystEngComm, 2014. 16(28): p. 6450-6458.

585   41.   Fang, F.-Q., et al., Anti-cancer effects of 2-oxoquinoline derivatives on the HCT116 and LoVo human colon cancer cell lines. Molecular medicine reports, 2015. 12(6): p. 8062-8070.

588   42.   Qin, H.-L., et al., Molecular docking studies and biological evaluation of chalcone based pyrazolines as tyrosinase inhibitors and potential anticancer agents. RSC Advances, 2015. 5(57): p. 46330-46338.

591   43.   Vichai, V. and K. Kirtikara, Sulforhodamine B colorimetric assay for cytotoxicity screening. Nature protocols, 2006. 1(3): p. 1112-1116.

593   44.   Patel, S., et al., In-vitro cytotoxicity activity of Solanum nigrum extract against Hela cell line and Vero cell line. International journal of pharmacy and pharmaceutical sciences, 2009. 1(1): p. 38-46.

596   45.   Abdelghani, E., et al., Synthesis and antimicrobial evaluation of some new pyrimidines and condensed pyrimidines. Arabian Journal of Chemistry, 2017. 10: p. S2926-S2933.

598   46.   Shakeel, A., Thiourea Derivatives in Drug Design and Medicinal Chemistry: A Short Review. Journal of Drug Design and Medicinal Chemistry, 2016. 2(1): p. 10.

27

600   47.   Zhao, C., et al., Pharmaceutical and medicinal significance of sulfur (S(VI))-Containing

601   motifs for drug discovery: A critical review. Eur J Med Chem, 2019. 162: p. 679-734.

602   48.   Baumgartner, B., et al., Green and highly efficient synthesis of perylene and naphthalene

603   bisimides in nothing but water. Chem Commun (Camb), 2017. 53(7): p. 1229-1232.

604   49.   Reinsch, H., "Green" Synthesis of Metal-Organic Frameworks. European Journal of

605   Inorganic Chemistry, 2016. 2016(27): p. 4290-4299.

606

List of Tables

Sample ID	v (C=O) cm^{-1}	v (N-H) str cm^{-1}
5-FU	1647.77	3409.02
5-FU-U (1A)	1633.23	3556.93, 3438.20
5-FU-U (1B)	1614.94	3437.62
5-FU-Th (2A)	1610.38	3599.96, 3493.97, 3376.24
5-FU-Th (2B)	1621.81	3568.20, 3388.06
5-FU-Ac (3A)	1663.09	3538.09, 3472.57
5-FU-Ac (3B)	1649.62	3499.40, 3555.67
5-FU-As (4A)	1678.63	3565.19, 3492.82
5-FU-As (4B)	1659.30	3496.39, 3560.13

611 **Table 2.** Percentage inhibition of cancer cells HCT-116 using different concentrations.

612

Sample ID	%age Inhibition of cancer cells HCT-116 using different concentrations			
	25 µg/mL	50 µg/mL	100 µg/mL	200 µg/mL
5FU	16.21±0.196	39.53±0.5585	54.28±0.5545	64.48±1.2113
1A	15.66±0.64	24.04±0.589	40.26±0.5832	31.60±0.5266
1B	14.57±0.566	30.97±0.5839	41.71±0.5835	45.72±0.5717
2A	13.48±0.589	18.21±0.6305	37.16±0.6305	50.46±0.5952
2B	29.33±0.8893	36.43±0.6008	51.91±0.5835	80.51±0.589
3A	13.84±0.5675	22.04±0.572	40.07±0.589	48.27±0.5775
3B	24.59±0.6014	35.15±0.6189	35.3±0.589	61.57±0.601
4A	25.68±0.5377	33.35±0.5952	50.27±0.589	68.31±0.5834
4B	12.02±0.5606	22.12±0.596	34.61±0.5832	59.56±0.8783

613

614

615

616

617 **Table 3.** Crystallite Size of 5-FU and Co-crystals using Scherrer equation [49].

618

Sample ID	2θ	Intensity	Θ	θ in Radians	Cos θ	FWHM	Crystallite Size (Aº)
5-FU	28.80º	1156	14.40	0.25	0.97	0.24	6.01
5-FU-U (1B)	28.19º	938	14.09	0.25	0.97	0.13	11.04
5-FU-Th (2B)	27.97º	5725	13.98	0.24	0.97	0.06	22.48
5-FU-Ac (3B)	29.10º	1249	14.55	0.25	0.97	0.051	27.85
5-FU-As (4B)	28.74º	2066	14.36	0.25	0.97	0.16	9.09

619

620

List of Figures
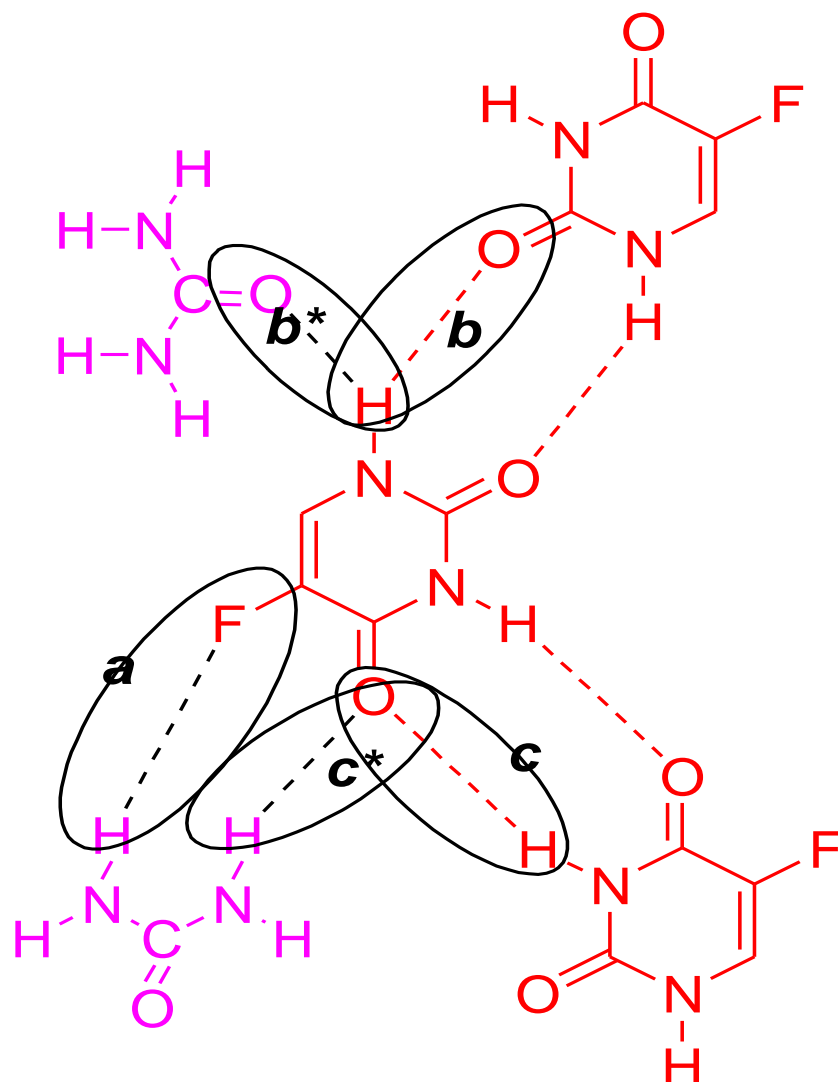
Fig. 1. Proposed interactions between 5-FU-U co-crystals.

627

628

629

630

631
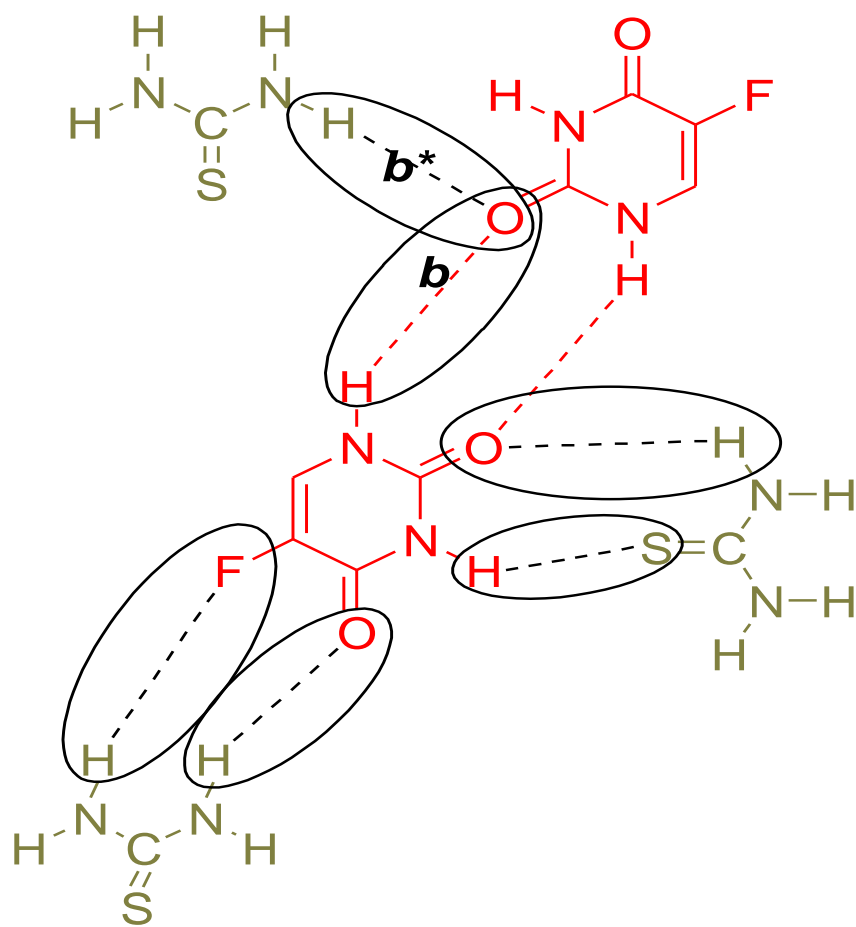
Fig. 2. Proposed interactions between 5-FU-Th co-crystals.

632

633

634

635

636

637

638

639

640
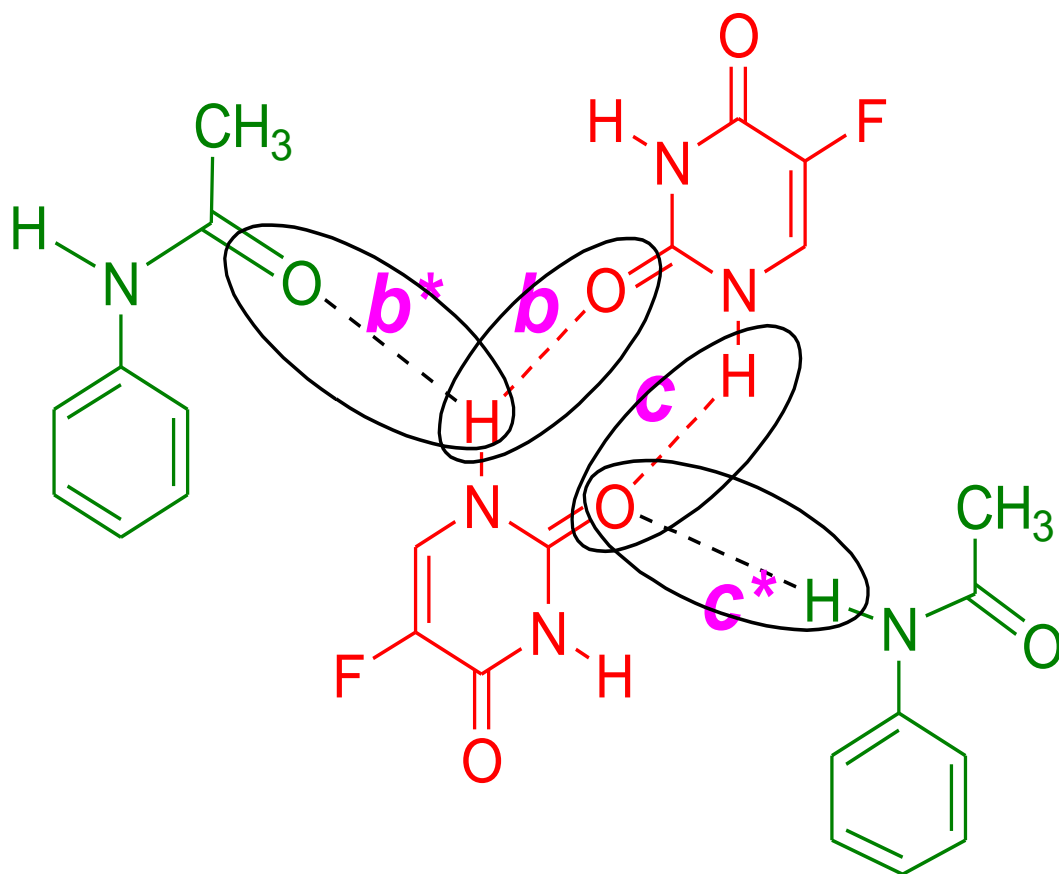
Fig. 3. Proposed interactions between 5-FU-Ac co-crystals.

641

642

643
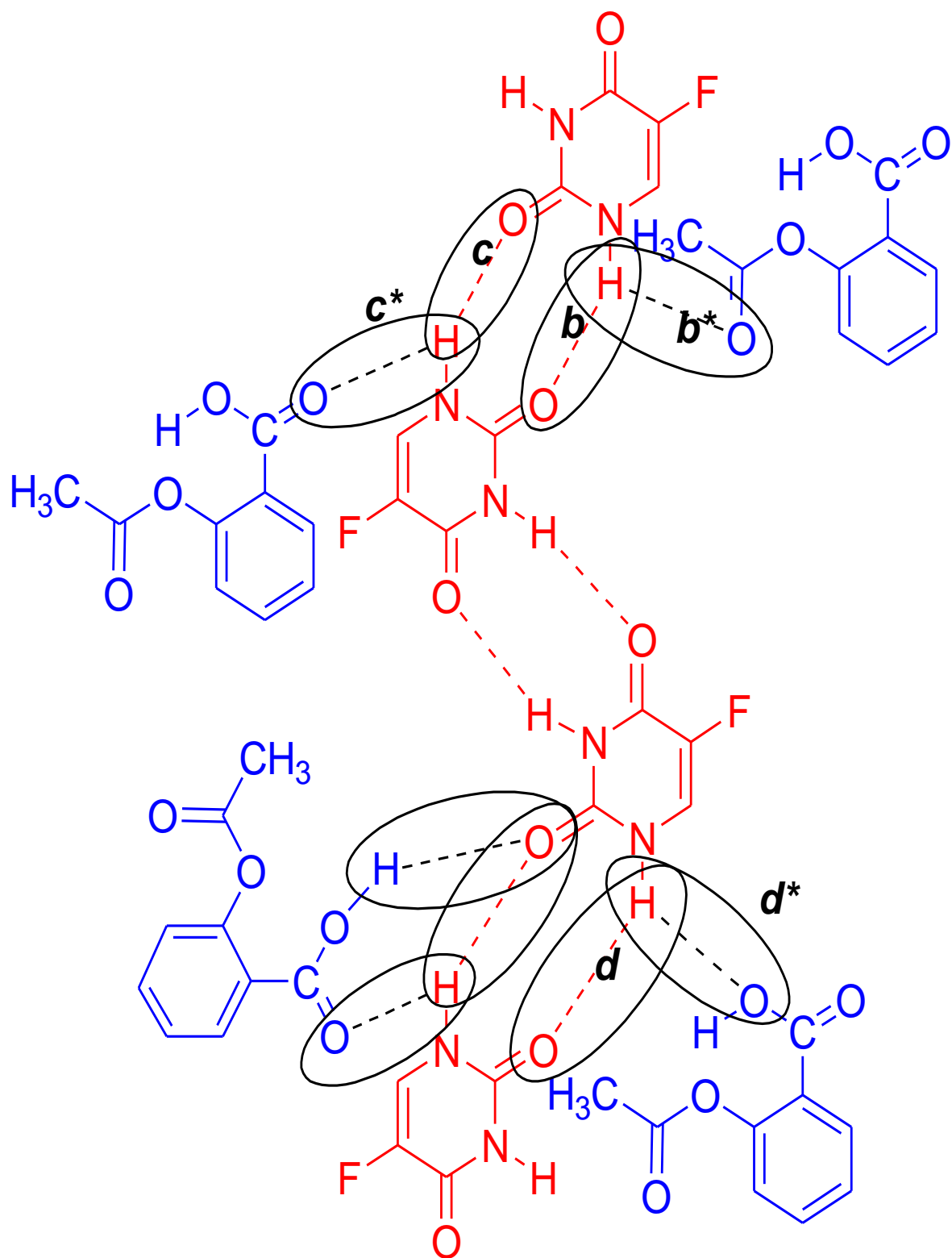
Fig. 4. Proposed interactions between 5-FU-As co-crystals.

647

648

649

650
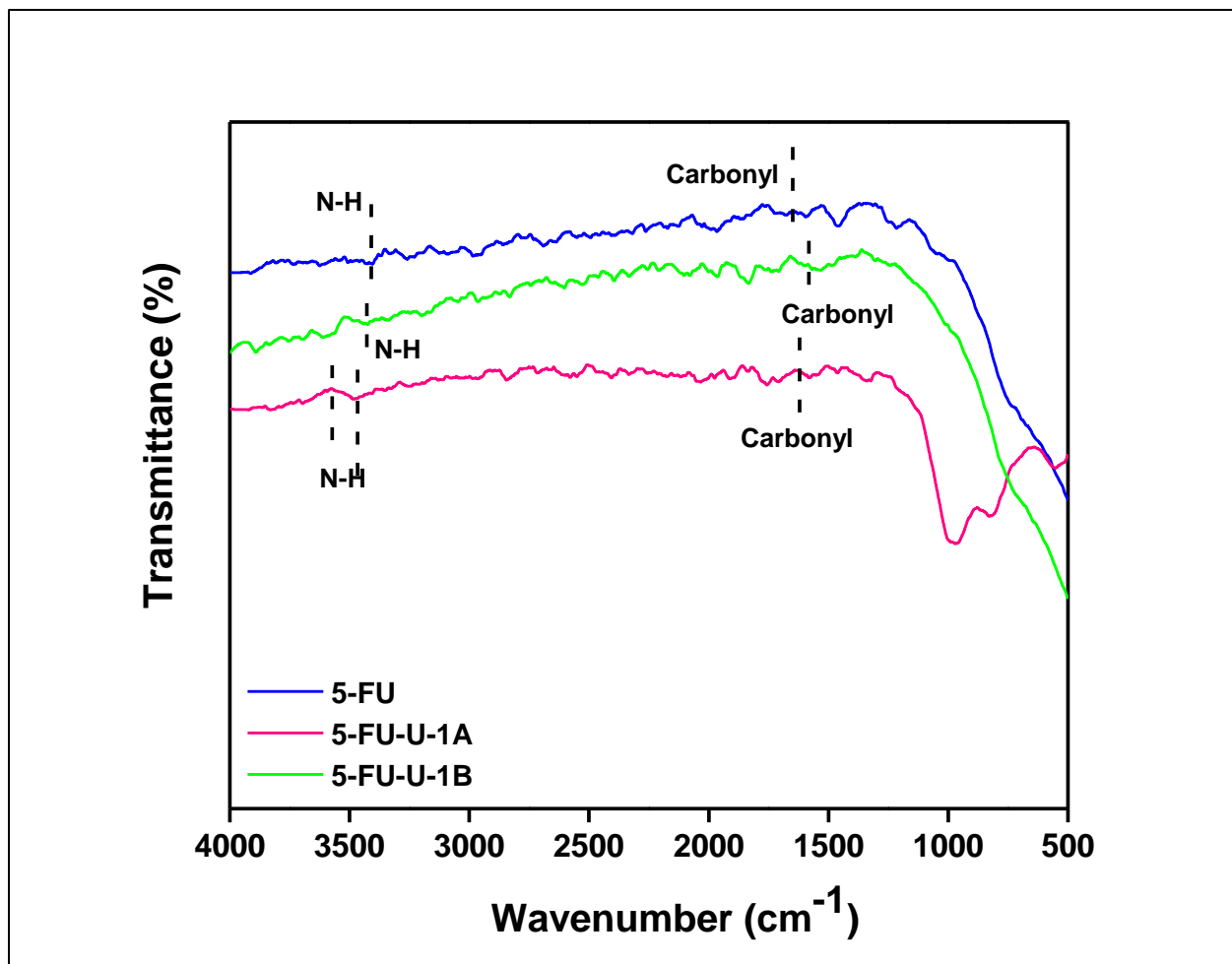
Fig. 5. Comparative FTIR spectra of 5-FU-U co-crystals fabricated by grinding (A) and solution (B) method.

654

655

656

657

658
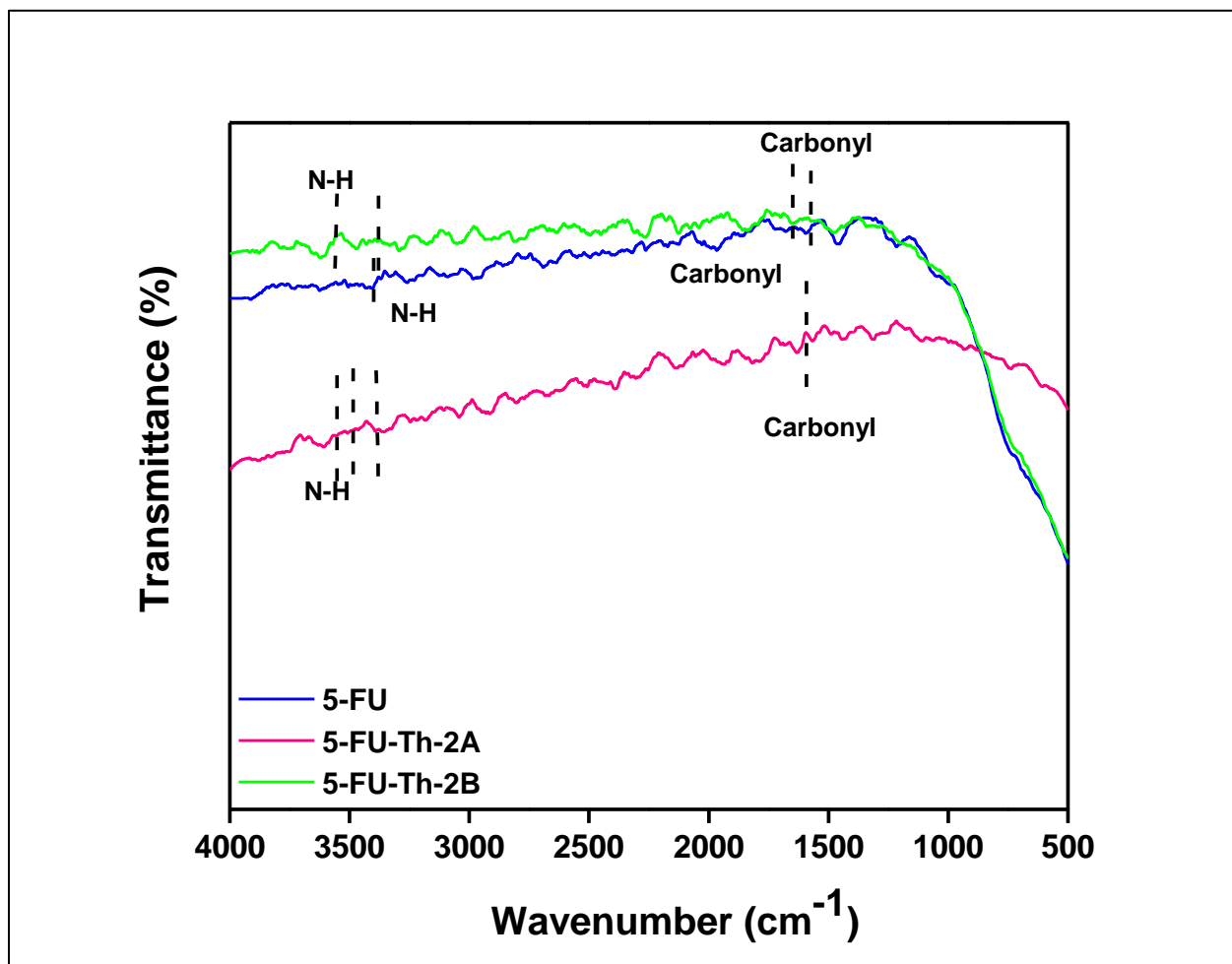
Fig. 6. Comparative FTIR spectra of 5-FU-Th co-crystals fabricated by grinding (A) and solution (B) method.

662

663

664

665

666

667
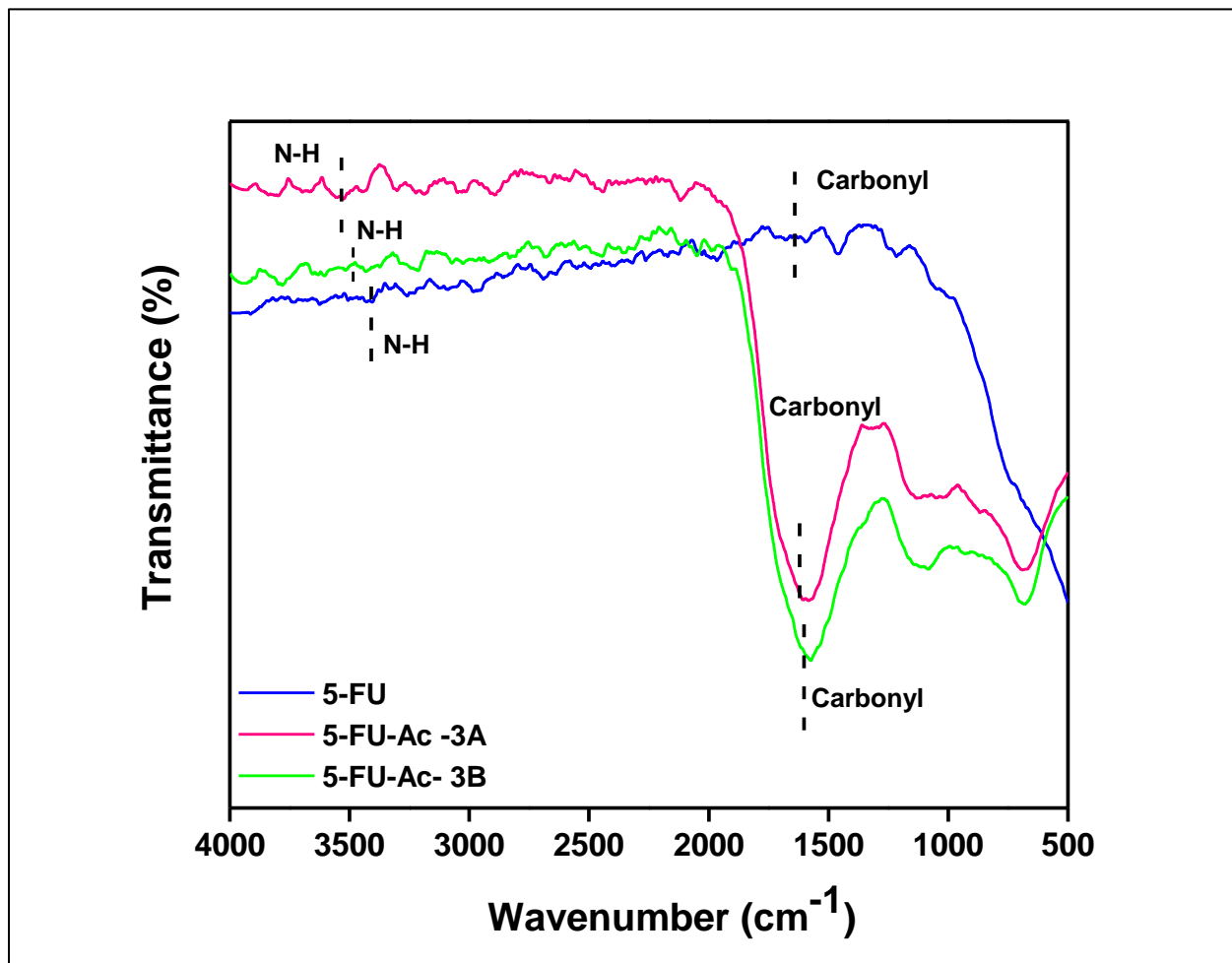
Fig. 7. Comparative FTIR spectra of 5-FU-Ac co-crystals fabricated by grinding (A) and solution
(B) method.

670

671

672

673

674
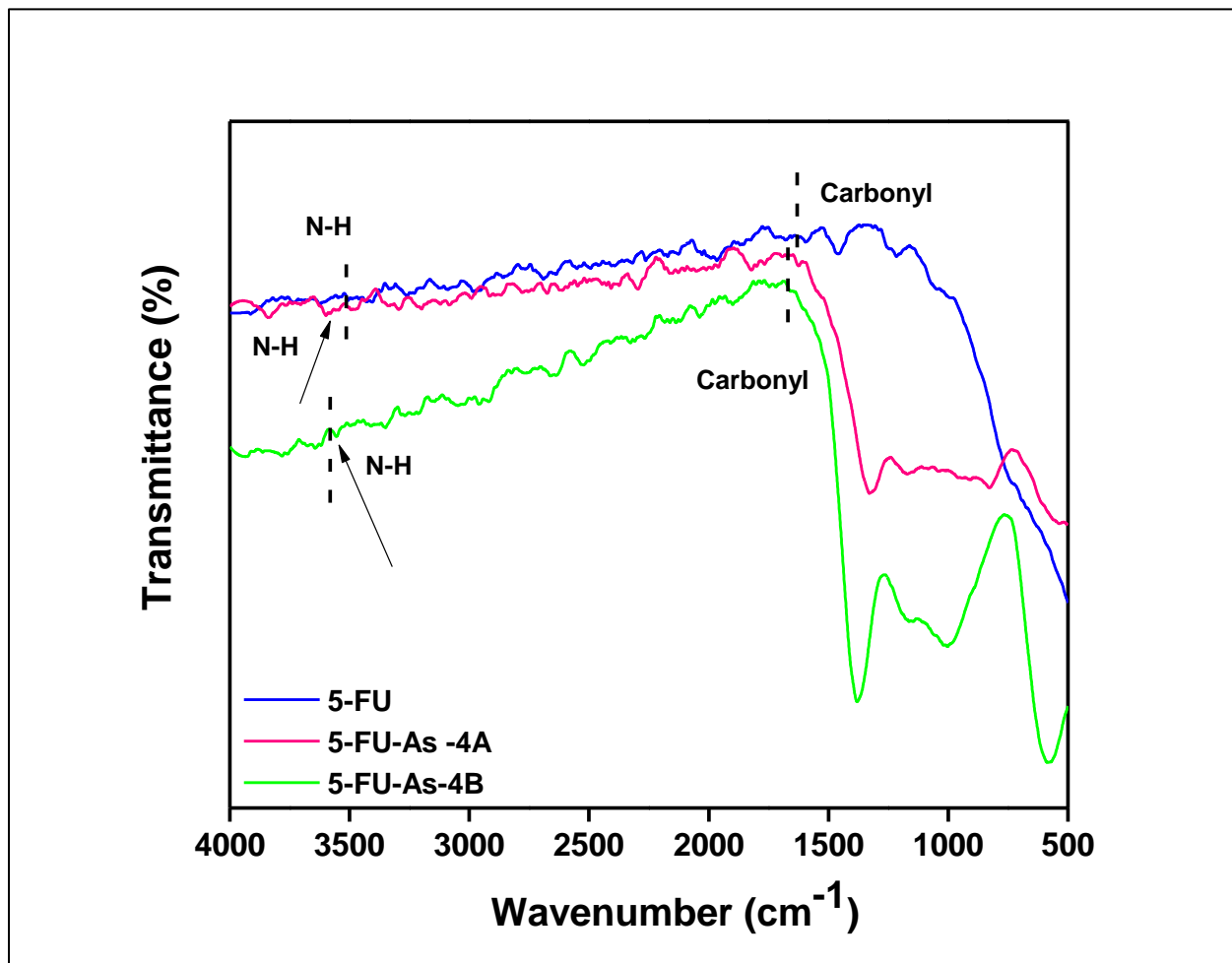
Fig. 8. Comparative FTIR spectra of 5-FU-As co-crystals fabricated by grinding (A) and solution (B) method.

678

679

680

681
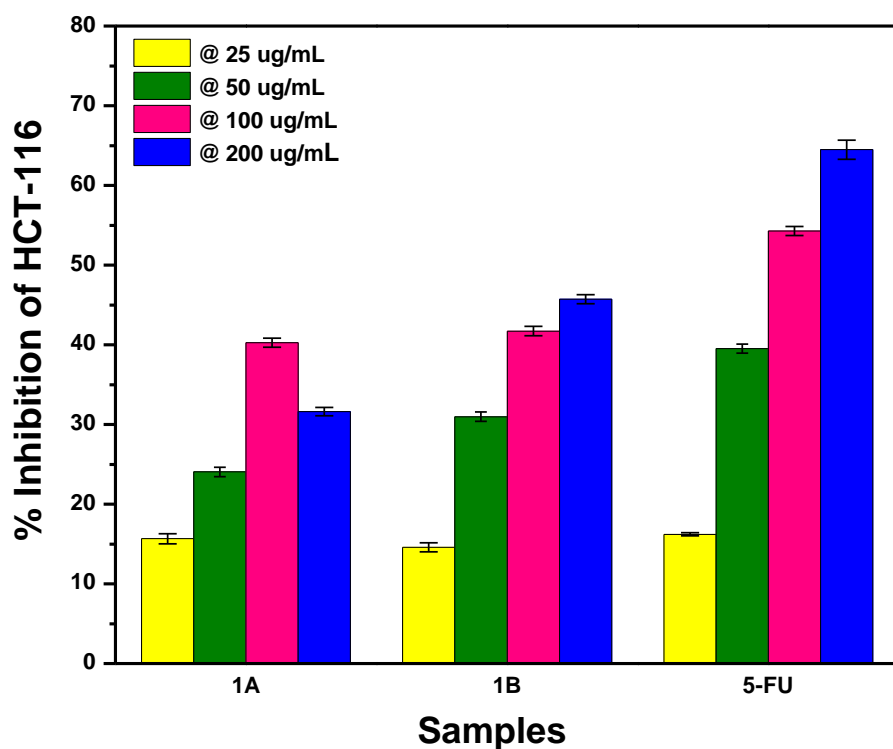
682

683

684 **Fig. 9.** Comparison of percentage growth inhibition of 5-FU-U co-crystals, fabricated by grinding
685 (A) and solution (B) method, at varying concentrations of actinimycetes against HCT 116
686 colorectal cell lines.

687

688

689

690

691

692
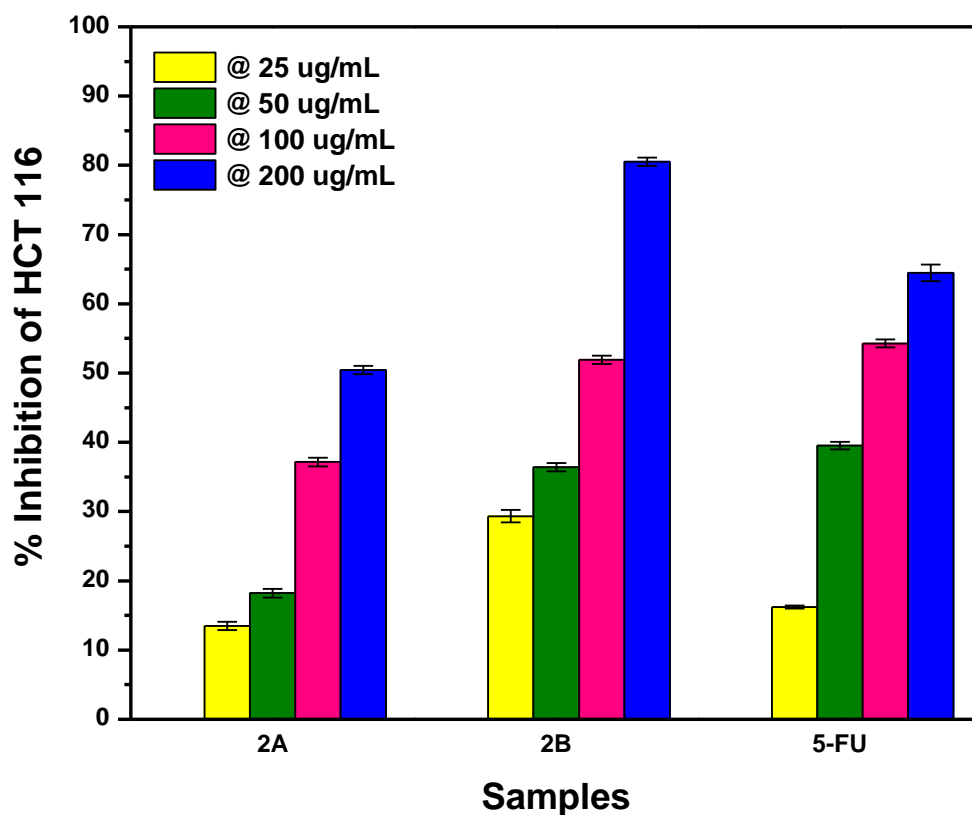
Fig. 10. Comparison of percentage growth inhibition of 5-FU-Th co-crystals, fabricated by grinding (A) and solution (B) method, at varying concentrations of actinimycetes against HCT 116 colorectal cell lines.

696

697

698

699

700

701

702

703

Fig. 11. Comparison of percentage growth inhibition of 5-FU-Ac co-crystals, fabricated by grinding (A) and solution (B) method, at varying concentrations of actinimycetes against HCT 116 colorectal cell lines.
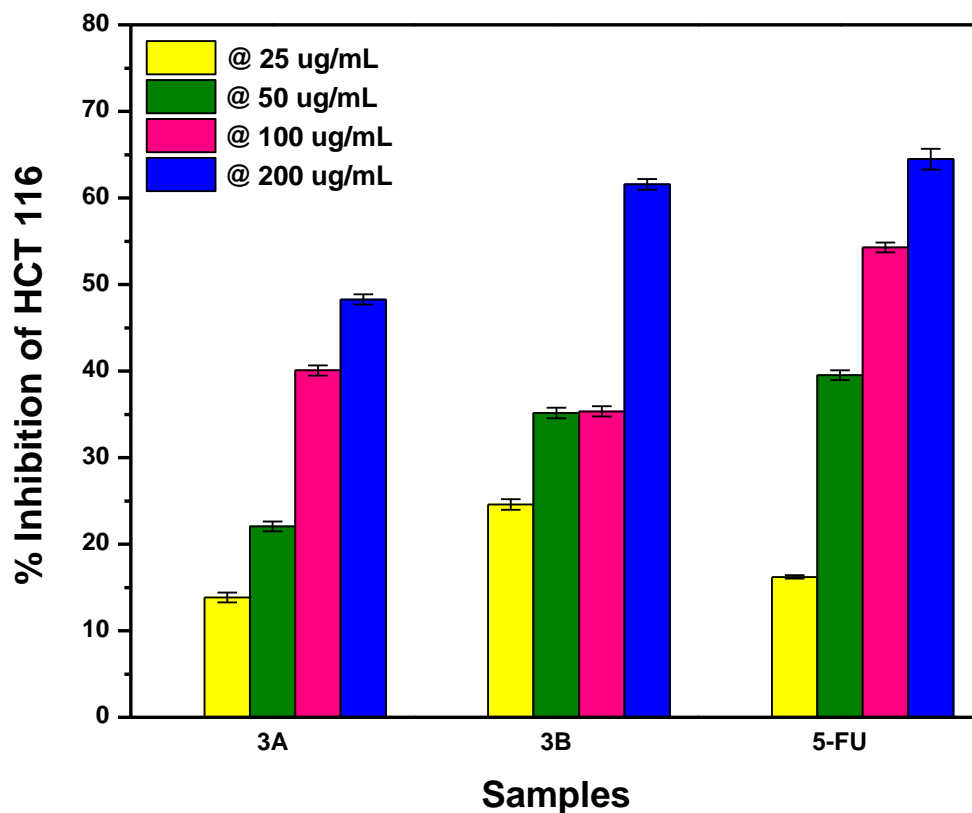
704

705
706
707

708

709

710

711

712

713

714

715
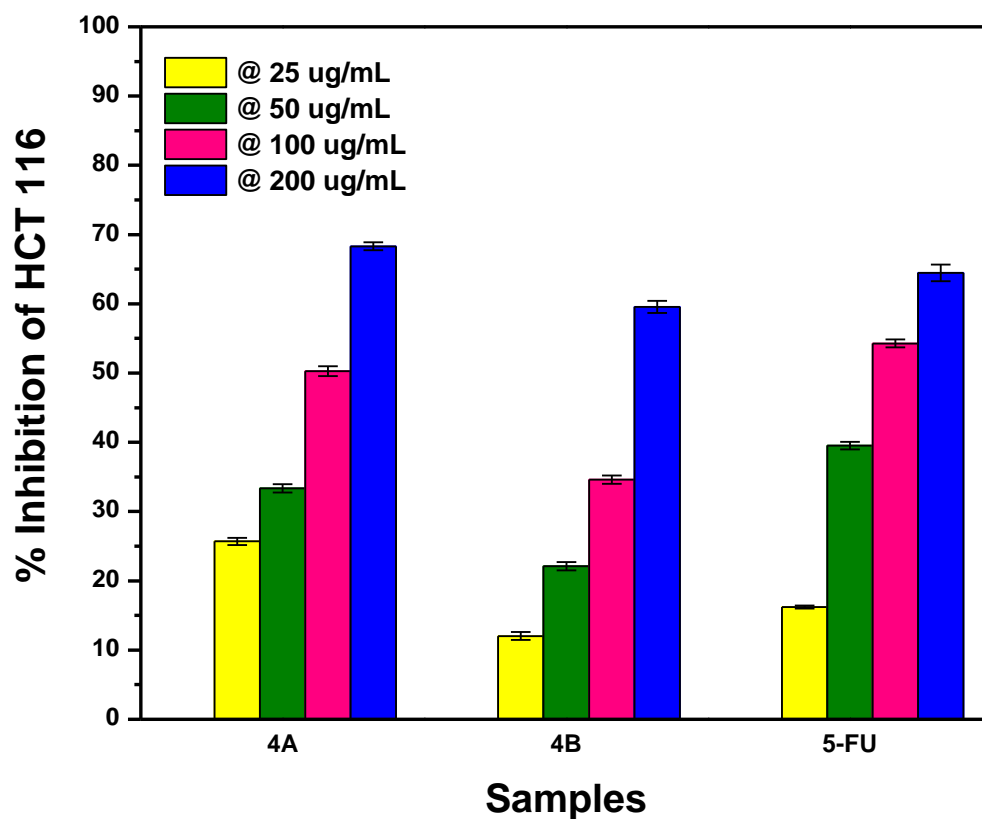
Fig. 12. Comparison of percentage growth inhibition of 5-FU-As co-crystals, fabricated by grinding (A) and solution (B) method, at varying concentrations of actinimycetes against HCT 116 colorectal cell lines.

720

721

722

723
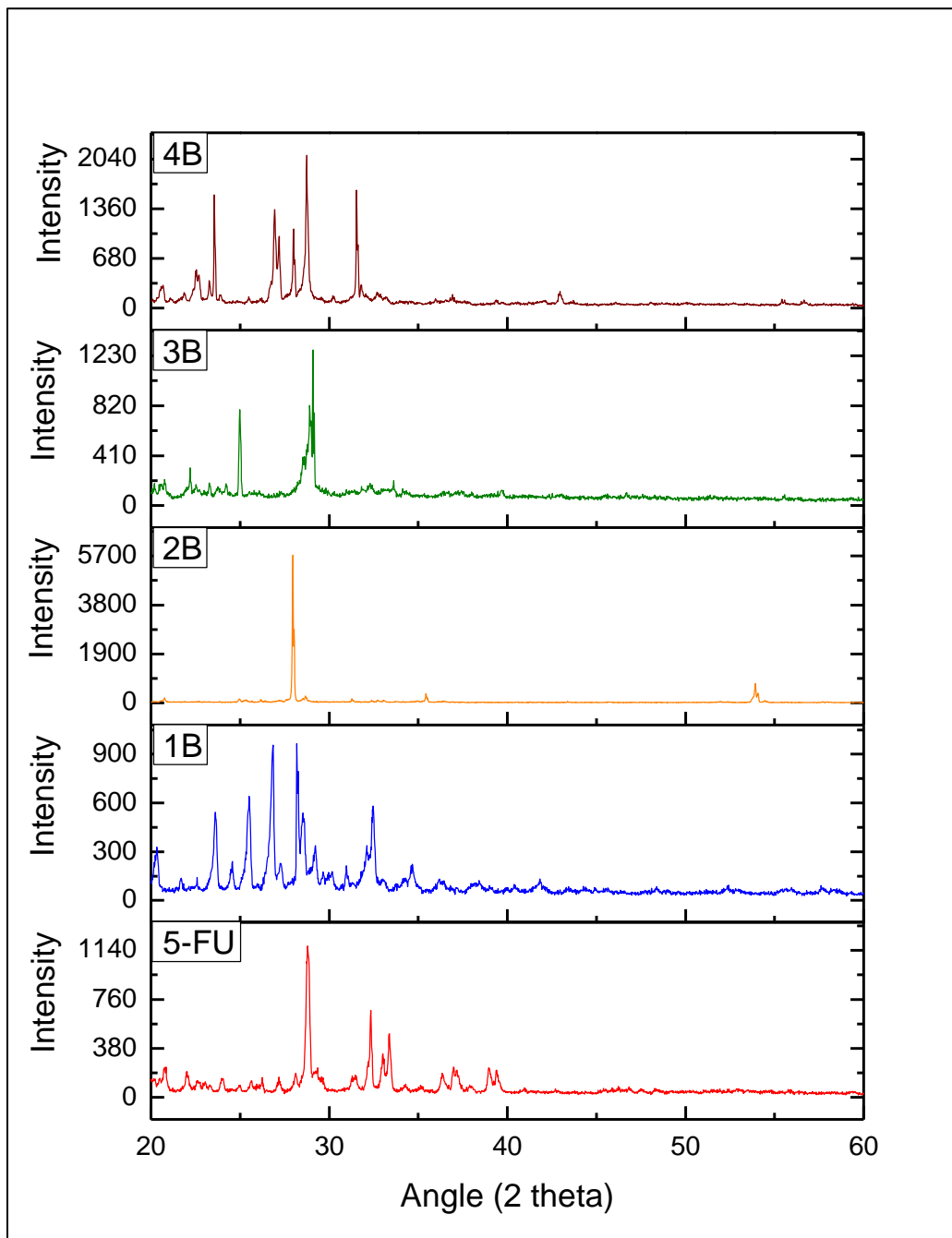
Fig. 13. Comparison of PXRD spectra of API and Co-formers fabricated by solution method (B).